

Enhanced coercivity and remanence of PrCo₅ nanoflakes prepared by surfactant-assisted ball milling with heat-treated starting powder*

Zuo Wen-Liang(左文亮)[†], Zhao Xin(赵鑫), Xiong Jie-Fu(熊杰夫), Shang Rong-Xiang(商荣翔), Zhang Ming(章明), Hu Feng-Xia(胡凤霞), Sun Ji-Rong(孙继荣), and Shen Bao-Gen(沈保根)[‡]

State Key Laboratory of Magnetism, Institute of Physics, Chinese Academy of Sciences, Beijing 100190, China

(Received 3 March 2015; revised manuscript received 30 March 2015; published online 18 May 2015)

PrCo₅ nanoflakes with strong texture and high coercivity of 8.15 kOe were prepared by surfactant-assisted ball milling with heat-treated starting powder. The thickness and length of the as-milled nanoflakes are mainly in the ranges of 50–100 nm and 0.5–3 μm, respectively. The x-ray diffraction patterns demonstrate that the heat treatment can increase the single phase and crystallinity of the PrCo₅ compound, and combined with the demagnetization curves, indicate that the single phase and crystallinity are important for preparing high-coercivity and strong-textured rare earth permanent magnetic nanoflakes. In addition, the coercivity mechanism of the as-milled PrCo₅ nanoflakes is studied by the angle dependence of coercivity for an aligned sample and the field dependence of coercivity, isothermal (IRM) and dc demagnetizing (DCD) remanence curves for an unaligned sample. The results indicate that the coercivity is dominated by co-existing mechanisms of pinning and nucleation. Furthermore, exchange coupling and dipolar coupling also co-exist in the sample.

Keywords: coercivity mechanism, textured PrCo₅ nanoflakes, surfactant-assisted ball milling, heat treatment

PACS: 71.20.Eh, 75.75.Cd, 75.30.Gw, 75.60.Jk

DOI: [10.1088/1674-1056/24/7/077103](https://doi.org/10.1088/1674-1056/24/7/077103)

1. Introduction

Nanostructured rare earth permanent magnetic (REPM) compounds with high coercivity and strong texture are important for obtaining high performance nanocomposite magnets and soft/hard exchange coupled magnets.^[1–3] Lately, the surfactant-assisted ball milling (SABM) method has been found to be efficient in the synthesis of textured nanostructured rare earth compounds,^[4] and many nanostructured Co-based rare earth permanent magnetic materials have been prepared by this method.^[5–10] In our recent work, we obtained a high coercivity of 7.8 kOe for PrCo₅ nanoflakes by low energy SABM.^[5] In fact, the largest advantage of low energy in the ball milling process is to prevent the destruction of the crystalline structure, which could be important for obtaining the high coercivity. Therefore, in the present work, the starting powder for milling was heat-treated for a week at 1173 K in order to obtain a high crystallinity. The x-ray diffraction patterns indicate that the heat treatment can increase the single phase and crystallinity of the PrCo₅ compound, and a larger coercivity of 8.15 kOe and a higher remanence ratio of 0.75 are obtained for the heat-treated sample.

2. Experiment

The PrCo₅ compound was prepared by arc melting in argon using pure metals. The ingots were melted five times to ensure homogeneity and then annealed at 1173 K for a week

under vacuum. The annealed ingots were ground down to less than 150 μm as the starting powder. The ball milling was performed for 8 h using GN-2 ball milling equipment (voltage was 60 V and the rotating speed was about 300 rpm). The weight ratio of balls to powder was 20:1. Oleylamine (80%–98%) and oleic acid (99%) were used as the surfactants. The total amount of the surfactants was 20% of the weight of the starting powder (oleylamine and oleic acid was 1:1). Heptane (99.8%) was used as the carrier liquid. The aligned PrCo₅ nanoflakes/resin composite was prepared by mixing the as-milled flakes with epoxy resin, and placing them into a 20 kOe magnetic field until the epoxy resin solidified. The phase structure was examined by x-ray powder diffraction (XRD) with Cu Kα radiation at room temperature. Morphology was characterized by scanning electron microscope (SEM). Magnetic properties were measured by a vibrating sample magnetometer with the maximum field of 20 kOe at room temperature.

3. Result and discussion

Figure 1(a) shows the measured XRD patterns of annealed and unannealed PrCo₅ powders. The unannealed sample crystallizes primarily in the CaCu₅-type hexagonal phase structure and with minor impurity. After being heat-treated at 1173 K for a week, the sample exhibits a single hexagonal phase structure (annealed). Meanwhile, the intensity and the

*Project supported by the National Basic Research Program of China (Grant No. 2014CB643702), the National Natural Science Foundation of China (Grant No. 51401235), and Beijing Natural Science Foundation, China (Grant No. 2152034).

[†]Corresponding author. E-mail: wlzuo@iphy.ac.cn

[‡]Corresponding author. E-mail: shenbg@aphy.iphy.ac.cn

width of the peaks become stronger and narrower, respectively, which indicates that the heat treatment can increase the single phase and crystallinity of the starting PrCo_5 powder. Figure 1(b) shows the demagnetization curves (DC) of annealed and unannealed PrCo_5 nanoflakes (unaligned). It can be seen that the annealed sample exhibits larger coercivity (8.15 kOe) and higher remanence ratio (0.75) than the unannealed sample, which indicates that the single phase and crystallinity of the starting PrCo_5 powder have an important influence on the final permanent magnetic performance of the nanoflakes. In order to further research the relationship between the magnetic properties and the crystallinity, the XRD patterns of annealed and unannealed PrCo_5 nanoflakes are shown in Fig. 1(c). It can be seen that both of the as-milled nanoflake samples exhibit only the hexagonal phase structure, which indicates that the phase structure can be kept during the milling process. It is noticed that the impurity cannot be observed for the unannealed sam-

ples after milling, which could be due to the low resolution of the XRD and the low content of the impurity. In addition, the stronger diffraction peaks of the annealed sample indicate that crystallinity can also be maintained well during the process of milling. Furthermore, the XRD pattern of the aligned sample also indicates a strong (0 0 l) out-of-plane alignment degree for the annealed sample (the easy magnetization directions along the c axis). In addition, the weaker diffraction peak ratio of (110)/(002) indicates that the heat treatment can further increase the alignment degree. An SEM image of nanoflakes for the annealed sample is shown in Fig. 1(d), the inset shows an enlarged image of a selected area. It can be seen that the thickness and the length of the nanoflakes are mainly in the ranges of 50–100 nm and 0.5–3 μm , respectively. Moreover, the nanoflakes spontaneously form a “kebab-like” morphology due to the c -axis texture and the magnetostatic interaction.

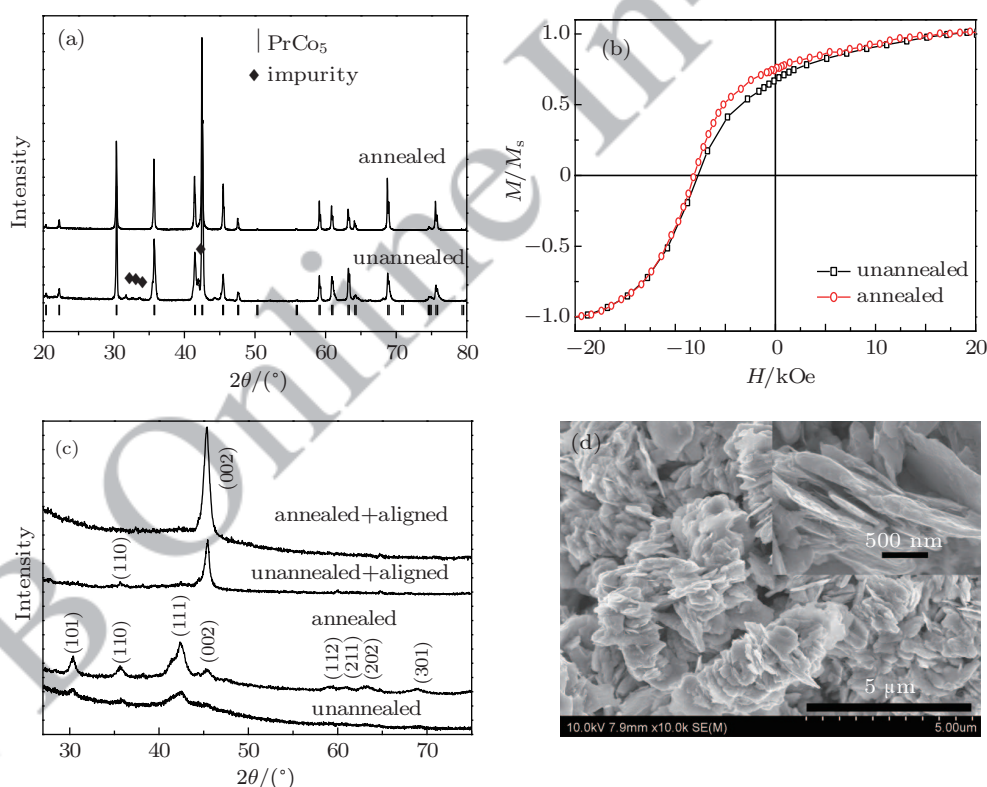


Fig. 1. (color online) (a) The XRD patterns of annealed and unannealed PrCo_5 powder. (b) The demagnetization curves of annealed and unannealed PrCo_5 nanoflakes (unaligned). (c) The XRD patterns of aligned annealed, aligned unannealed, unaligned annealed, and unaligned unannealed PrCo_5 nanoflakes. (d) The SEM image of nanoflakes for the annealed sample, the inset is the enlarged image of the selected area.

All the following analysis pertains only to the annealed samples, unless stated otherwise. Figure 2(a) shows the angular dependence of the half-hysteresis loop for the aligned PrCo_5 nanoflakes/resin composite, where the external field is applied at a certain angle θ with respect to the magnetically aligned axis of the sample. It can be seen that M_r/M_s reaches 0.89 for the sample with $\theta = 0^\circ$, which indicates that the sam-

ple has a good alignment degree. In order to more accurately describe the alignment degree, we also calculate the average misalignment angle, $\varphi = \arctan[2M_r(\perp)/M_r(\parallel)]$,^[6,11] where $M_r(\perp)$ and $M_r(\parallel)$ are the remanence of the perpendicular and parallel directions of the easy axis, respectively. The misalignment angle φ is 31° , which is comparable with the experimental results of ball milling in a magnetic field,^[6] which also

confirms that the nanoflakes have a high texture degree. In addition, H_c first increases and reaches 8.9 kOe at 60° and then decreases with the angle θ increasing. This phenomenon of H_c first increasing then decreasing is also observed for many rare earth permanent magnetic materials.^[12–17] However, this phenomenon has been explained from many viewpoints, for example, defect-region associated reversed nucleus,^[12] nucleation mechanism with consideration of the anisotropy constant K_2 and misalignment of the grains,^[13] domain-wall propagation allowing for moment rotation,^[14] the starting field theory taking into account the intergrain interaction,^[15] co-existing pinning and nucleation,^[16] surface defects determining pinning or nucleation,^[17] and nucleation by curling.^[18] The many different theories arise due to the experimental results which usually lie between the theoretical predictions of Kondorsky domain wall pinning ($1/\cos\theta$) and Stoner–Wohlfarth coherent rotation (see Fig. 2(b)). Furthermore, the interaction of grain, defect, and misalignment are inevitable in the actual magnet.

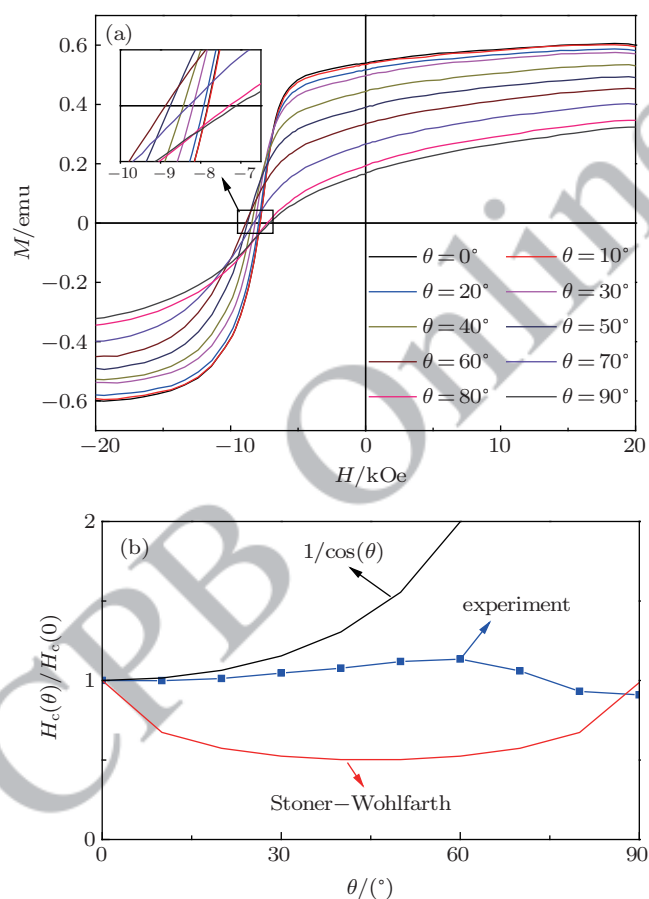


Fig. 2. (color online) The angular dependence of (a) half-hysteresis loop and (b) $H_c(\theta)/H_c(0)$ for the aligned PrCo_5 nanoflakes/resin composite.

In order to further clarify the coercivity mechanism and the possible interaction of PrCo_5 nanoflakes, the minor hysteresis loops and recoil loops of the unaligned PrCo_5 nanoflakes resin composite are measured and shown in Figs. 3(a) and 3(b), respectively. The inset of Fig. 3(a) shows

the normalization of coercivity dependence of the maximum applied field, which is determined from the minor hysteresis loops. It can be seen that the coercivity changes slowly at the low applied fields ($H \leq 3$ kOe, $H/H_{\text{cmax}} < 0.5$) and then increases quickly when the applied field is larger than 3 kOe until 13.8 kOe ($H/H_{\text{cmax}} = 1.7$). This characteristic cannot be completely decided by only pinning or nucleation. Therefore, we think that the coercivity may be dominated by co-existing mechanisms of both pinning and nucleation.

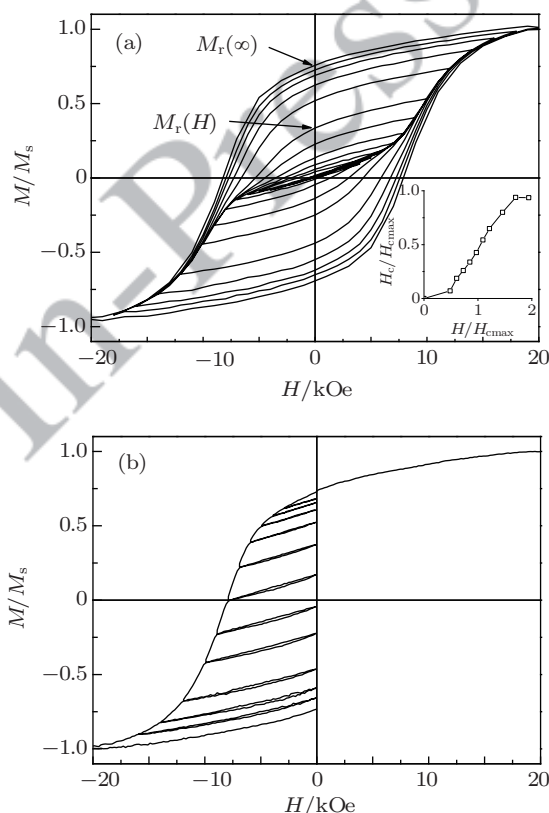


Fig. 3. (a) The minor hysteresis loops and (b) recoil loops of the unaligned PrCo_5 nanoflakes/resin composite, the inset is the normalization of coercivity dependence on the applied field.

It is known that Henkel plots are very important and useful in checking the interaction of particles and the magnetization reversal mechanism, which is defined as $\delta M = M_d(H) - [1 - 2M_r(H)]$. Here $M_r(H)$ is the isothermal (IRM) remanence (normalized to $M_r(H)/M_r(\infty)$) acquired after the application and subsequent removal of field H , $M_d(H)$ is dc demagnetizing (DCD) remanence (normalized to $M_d(H)/M_r(\infty)$) acquired after saturation in one direction and subsequent application and removal of a direct field H in the reverse direction. The two remanence curves of IRM and DCD are shown in Fig. 4(a), and the data are from the Figs. 3(a) and 3(b), respectively. Many studies have indicated that the IRM and DCD remanence curves can reveal the irreversible energy barrier distribution information, and the domain wall pinning energy distribution can be determined by the differentiation of the IRM curve, while both the domain wall pinning and the nucleation

energy distribution can be determined by the differentiation of the DCD curve.^[19,20] Therefore, it is also practical for the two-coercivity model. Figure 4(b) shows the differentiation curves of the IRM and DCD remanence (normalizing the area of the curves to unity). It can be seen that both energy barrier distributions show a single peak at about 8.2 kOe, and the differential peak of IRM shifts slightly to the right. The results indicate that, in the magnetization reversal process, the reversal domain nucleation first appears, and then both nucleation and the pinning effect occur immediately. Furthermore, a very large overlap of energy barrier distributions can be observed. This large overlap could be due to the overlap of the nucleation and the domain wall pinning energy barrier distribution.^[19] And it also indicates that nucleation and pinning co-exist in the magnetization reversal processes. In addition, both differentiation curves of the IRM and DCD remanence show a broad peak, which can also further lead to the overlap of the energy barrier distribution and is usually caused by the demagnetizing effects.^[19] Moreover, the interaction effects in particulate magnetic materials can be studied via the Wohlfarth relation: $M_d(H) = 1 - 2M_r(H)$,^[19-23] which also means $\delta M = 0$. Therefore, any $\delta M \neq 0$ in experimental data can be attributed to the effect of interaction. The positive δM implies that the interaction attempts to magnetize the materials and is usually associated with exchange coupling, while negative δM means that the interaction attempts to demagnetize the materials and is usually associated with dipolar coupling. It can be seen from Fig. 4(c) that δM shows positive values at low magnetic field while negative values at high magnetic field, which indicates that the main interaction of nanoflakes is exchange coupling in low magnetic field and dipolar coupling in high magnetic field. This characteristic is also demonstrated by using scanning transmission x-ray microscopy for Nd-Fe-B nanocrystalline magnets.^[24] In addition, the flatness of the $M_r(H)$ and DM curves (see Fig. 4(a), DM from Fig. 1(b)) also demonstrates the exchange-spring behaviors.^[25] The fact that the remanence magnetic ratio is larger than 0.5 for the unaligned sample (see Fig. 1(b)) indicates that the nanoflakes have a spontaneous remanence enhancement effect due to the exchange interaction.^[5] Moreover, dipolar coupling can also be demonstrated by the spontaneous formation of the kebab-like morphology for the as-milled nanoflakes due to the magnetostatic interaction (see Fig. 1(c)). A negative δM (dipolar coupling) attempts to demagnetize the materials, which could decrease the coercivity of the as-milled PrCo₅ nanoflakes. In addition, we find that δM shows negative values for the as-milled Pr-Fe-B nanoflakes under any field,^[26] which could explain the relatively low coercivity of R₂Fe₁₄B (R=Pr, Nd) nanoflakes, in contrast with the high coercivity of RCo₅ (R=Pr, Sm) nanoflakes. Therefore, decreasing the negative effect of dipolar coupling could

be very useful for obtaining relatively high coercivity.

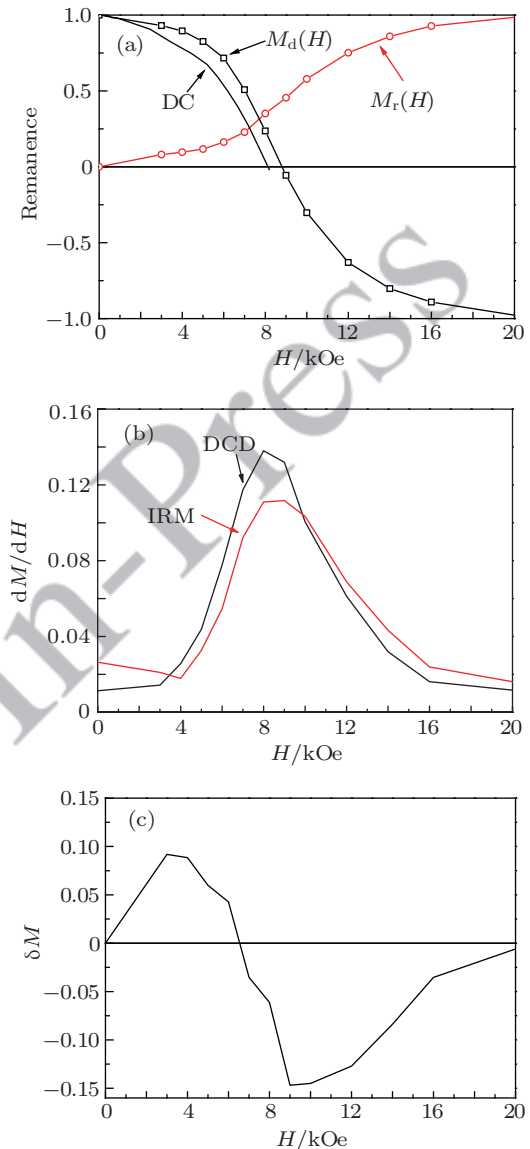


Fig. 4. (color online) (a) The field dependence of the DC curves, IRM and DCD remanence curves, (b) the differentiation curves of the IRM and DCD remanence, (c) Henkel plots of unaligned PrCo₅ nanoflakes.

4. Conclusion

The large coercivity of 8.15 kOe and high remanence ratio of 0.75 for PrCo₅ nanoflakes, achieved by surfactant-assisted ball milling of heat-treated starting powder, is the maximum coercivity for PrCo₅ nanoparticles or nanoflakes until now. The x-ray diffraction patterns demonstrate that the heat treatment can increase the single phase and crystallinity of the PrCo₅ compound, and the single phase and crystallinity are important for preparing rare earth permanent magnetic nanoflakes with high coercivity and strong texture. In addition, the angle dependence of coercivity for an aligned sample and the field dependence of coercivity, isothermal and dc demagnetizing remanence curves for an unaligned sample indicate that the coercivity is dominated by co-existing mechanisms of

pinning and nucleation. Furthermore, the further analysis indicates that the exchange coupling and dipolar coupling also co-exist in the samples.

References

- [1] Sun S, Murray C B, Weller D, Folks L and Moser A 2000 *Science* **287** 1989
- [2] Zeng H, Li J, Liu J P, Wang Z L and Sun S 2002 *Nature* **420** 395
- [3] Akdogan N G, Hadjipanayis G C and Sellmyer D J 2009 *IEEE Trans. Magn.* **45** 4417
- [4] Chakka V M, Altuncevahir B, Jin Z Q, Li Y and Liu J P 2006 *J. Appl. Phys.* **99** 08E912
- [5] Zuo W L, Liu R M, Zheng X Q, Wu R R, Hu F X, Sun J R and Shen B G 2014 *J. Appl. Phys.* **115** 17A728
- [6] Rong C B, Nguyen V V and Liu J P 2010 *J. Appl. Phys.* **107** 09A717
- [7] Yu N J, Pan M X, Zhang P Y, Ge H L and Wu Q 2015 *J. Magn. Magn. Mater.* **378** 107
- [8] Wang W Q, Hu X J, Li X H, Huang G W, Zhang Y M and Zhang X Y 2014 *J. Alloys Compd.* **589** 283
- [9] Nie J W, Han X H, Du J, Xia W X, Zhang J, Guo Z H, Yan A R, Li W and Liu J P 2013 *J. Magn. Magn. Mater.* **347** 116
- [10] Shen Y, Huang M Q, Higgins A K, Liu S, Horwath J C and Chen C H 2010 *J. Appl. Phys.* **107** 09A722
- [11] Fernengel W, Lehnert A, Katter M, Rodewald W and Wall B 1996 *J. Magn. Magn. Mater.* **157/158** 19
- [12] Bernasconi J, Strässler S and Perkins R S 1975 *AIP Conference Proceedings* **24** 761
- [13] Kronmüller H, Durst K D and Martinek G 1987 *J. Magn. Magn. Mater.* **69** 149
- [14] Elbaz D, Givord D, Hirosawa S, Missell F P, Rossignol M F and VillasBoas V 1991 *J. Appl. Phys.* **69** 5492
- [15] Gao R W, Zhang D H, Zhang Y M, Li W, Wang Y S and Yu X J 2001 *J. Magn. Magn. Mater.* **224** 125
- [16] Panagiotopoulos I, Gjoka M and Niarchos D 2004 *J. Magn. Magn. Mater.* **279** 389
- [17] Bance S, Oezelt H, Schrefl T, Ciuta G, Dempsey N M, Givord D, Winkelhofer M, Hrkac G, Zimanyi G, Gutfleisch O, Woodcock T G, Shoji T, Yano M, Kato A and Manabe A 2014 *Appl. Phys. Lett.* **104** 182408
- [18] Aharoni A 1997 *J. Appl. Phys.* **82** 1281
- [19] Thomson T and O'Grady K 1997 *J. Phys. D: Appl. Phys.* **30** 1566
- [20] Wang J B, Liu Q F, Xue D S and Li F S 2004 *Chin. Phys. Lett.* **21** 945
- [21] Speliotis D E and Lynch W 1991 *J. Appl. Phys.* **69** 4496
- [22] Mitchler P D, Dan Dahlberg E, Engle E and Roshko R M 1995 *IEEE Trans. Magn.* **31** 2499
- [23] Garca-Otero J, Porto M and Rivas J 2000 *J. Appl. Phys.* **87** 7376
- [24] Ohtori H, Lwano K, Mitsumata C, Yano M, Kato A, Shoji T, Manabe A and Ono K 2014 *J. Appl. Phys.* **115** 17A717
- [25] Liu J P, Liu Y and Sellmyer D J 1998 *J. Appl. Phys.* **83** 6608
- [26] Zuo W L, Zhang M, Niu E, Shao X P, Hu F X, Sun J R and Shen B G 2015 *J. Magn. Magn. Mater.* **390** 15